HMG-CoA Reductase Inhibition Causes Increased Necrosis and Apoptosis in an *In Vivo* Mouse Glioblastoma Multiforme Model

SIMON R. BABABEYGY[1,2], NIKA V. POLEVAYA[1], SAWSAN YOUSSEF[3], AMY SUN[1],
ANMING XIONG[1], TIFFANY PRUGPICHAILERS[1], ANAND VEERAVAGU[1],
LEWIS C. HOU[1], LAWRENCE STEINMAN[3] and VICTOR TSE[1,4]

[1]Department of Neurosurgery, Stanford University Medical Center, Stanford, CA 94305;
[2]Howard Hughes Medical Institute,
[3]Department of Neurology and Neurological Sciences,
Stanford University School of Medicine, Stanford, CA 94305;
[4]Kaiser Neurosurgery, Redwood City, CA, 94063, U.S.A.

Abstract. *Background: Statins are thought to have tumorolytic properties, reducing angiogenesis by inhibiting pro-angiogenic factors and inducing apoptosis of mural pericytes within the tumor vascular tree. Materials and Methods: An orthotopic mouse glioblastoma (GL-26) model was used to investigate the effect of simvastatin on glioblastoma vasculature in vivo. GL-26 cells were implanted into the striatum of C5LKa mice treated with either control, low- or high-dose simvastatin. Brains were analyzed for necrotic volume, apoptosis, morphology and pericytic cells within the vascular tree. Results: Low-dose simvastatin increased necrosis and apoptosis compared to both control and high-dose simvastatin groups. High-dose simvastatin increased vessel caliber by reducing pericytic cells along the tumor vessel wall compared to both control and low-dose simvastatin groups. Conclusion: Simvastatin has a dual effect on tumorigenesis. At high doses, it may worsen instead of 'normalizing' tumor angio-architecture, albeit low doses affect tumor cell survival by promoting necrosis and apoptosis.*

Statins such as simvastatin, lovastatin and cerivastatin competitively inhibit HMG-CoA reductase, which reduces overall cholesterol levels (1). The potential tumorolytic properties of these statins have been noted for a decade. It has been reported that simvastatin can inhibit growth and migration of human glioma cells both *in vitro* (2) and *in vivo*

Correspondence to: Victor Tse, MD, Ph.D., Department of Neurosurgery, Stanford University Medical Center, 1201 Welch Road, P310, Stanford, CA 94305-5327, U.S.A. Tel: +1 6507235574, Fax: +1 6507237813, e-mail: tsevictor@gmail.com

(3), as well as cause apoptosis (3, 4). Simvastatin up-regulates protein kinase C in rat glioma cells, which correlates negatively with glioma growth rate (5). Other studies have demonstrated the potential benefits of simvastatin therapy for glioma in conjunction with other antitumor agents such as carmustine and beta-interferon (6, 7), where simvastatin also reduced cell proliferation. Emerging studies have shown that statins affect tumor angiogenesis by blocking the action of pro-angiogenic factors (8) and induce apoptosis of the mural pericytes within the tumor vascular tree (9). Additionally, pravastatin inhibits tubular formation in human umbilical vein endothelial cells by blocking their adhesion to extracellular matrix (10). Collectively, these data form the basis of this study to investigate the effect of simvastatin on vascular architecture and proliferation of glioblastoma both *in vivo* and *in vitro*.

Materials and Methods

Animal model and surgery. A subclone of mouse glioblastoma (GL-26) cell line was adapted to grow in C5LKa mice. GL 26 cells were grown in Dulbecco's modified Eagle's medium (DMEM; Gibco, Gaithersburg, MD, USA) with 1% penicillin/streptomycin and 10% fetal calf serum (Gibco). These tumor cells had a 98.5% plating efficiency with a duplicating time of 31.34±3.72 hours. *In vivo*, these tumor cells formed solid tumor with the same morphology and histology resembling that of human glioblastoma multiforme (GBM), an orthotopic brain tumor model as previously reported (11). Mice were anesthetized with an intramuscular injection of ketamine (22-44 mg/kg), xylazine (2.5 mg/kg), and acepromazine (0.75 mg/kg). A total of 1×10^5 GL-26 cells in 5 μl were implanted stereotactically into the left striatum of the animal using a mouse stereotactic frame (Kopf Instruments, Tujunga, CA, USA) under a surgical protocol approved by the Administrative Panel on Laboratory Animal Care at Stanford University, USA. Twenty-six animals were used for the survival study. Animals were euthanized when they were moribund according to the protocol approved by our Administrative Panel on Laboratory Animal Care.

Simvastatin treatment. Mice were divided into three treatment groups: control (PBS-treated), low-dose simvastatin (1 mg/kg/day; CalBiochem, La Jolla, CA, USA) and high-dose simvastatin (10 mg/kg/day) as previously described (12, 13); 1 ml solution was administered daily *via* oral gavage, starting on postoperative day (POD) one. Upon becoming moribund, animals were perfused, their brains excised and immunohistochemistry was performed on brain sections. Imaging analysis (necrotic cavity measurement) was performed using Simple PCI software. For frozen section preparation, prepared perfused brains (as previously described) were cut at 12 μm thickness on a cryostat (Leica CM 3000; Leica, Germany) at –15˚C. Tumor size, vascular density, vessel caliber and survival in treatment and non-treatment groups were measured as previously described (14). Statistical significance was determined by using two-way ANOVA and Student's *t*-test.

Immunohistochemistry. For immunofluorescence staining and epifluorescence microscopy, animals were perfused intracardially with cold PBS (Invitrogen, USA) and 0.01 M EDTA (Invitrogen), followed by 4% neutral paraformaldehyde at 4˚C. Brains were stored in 4% paraformaldehyde for 3 days, and subsequently dehydrated in 30% sucrose for 3 days. Brains were then cut into 20 μm serial sections on a freezing microtome (Microm HM450; Thermo Scientific, Waltham, MA, USA). Sections were stored at –20˚C in tissue cryoprotectant solution and removed for immunohistochemistry. Sections were stained for endothelial cells with CD31 (primary antibody, rat anti-mouse, 1:100; Jackson ImmunoResearch, USA) and Cy3-labled secondary antibody (donkey anti-rat, 1:250; Chemicon, CA, USA). Sections were mounted and counterstained with Vectashield with DAPI (H-1500; Vector Laboratories, CA, USA) and examined with Nikon epifluorescent microscope (Eclipse 80i; Nikon, Tokyo, Japan). Images were digitally recorded with Advanced PCI software (Compix Inc., PA, USA) under ×100 and ×200 power. Four sections were examined per animal, and four quadrants were imaged per section. Vascular density was determined by analyzing 280 slide sections and 836 vessels, and expressed as number of vessels/mm^2 (mean±SD). The diameter of vessels was defined as the smallest vector measurement between two edges of an outlined blood vessel. To determine tumor size, sections were counterstained with crystal violet in anatomical order. The area of the sections was determined using Advanced PCI software. The sum of the sectional areas was then multiplied by the sectional thickness (20 μm), and the resulting tumor size was expressed in mm^3. Statistical analysis was performed using Graph Prism software (San Diego, CA, USA). Pericytes were visualized and counted by immunostaining with NG-2 (1:50, Chemicon) as the pericytic marker. The vascular tree in this part of the study was visualized by using FITC–conjugated tomato lectin (1:200; Vector Laboratories).

TUNEL apoptosis assay. In separate experiments, human umbilical vein endothelial cells (HUVECs) and GL-26 cells of each type were grown on coverslips in 6-well plates for 3 days to produce a 80-90% confluent layer in media containing DMEM with 1% penicillin/ streptomycin, and 10% fetal calf serum (Gibco). Three days later, when the confluent layer was obtained, cells were washed from old media twice by adding 1 × PBS to the coverslips, then fresh media were added with either 1 or 10 μM purified active simvastatin (sodium salt; CalBiochem), or with vehicle (PBS only). Cells were incubated for 24, 48 and 72 hours and at each time point 3 coverslips were taken from each treatment and washed with PBS twice. Terminal deoxynucleotidyl transferase biotin-

dUTP nick end-labeling (TUNEL) assay was performed on these slides using ApopTag® Peroxidase *In Situ* Apoptosis Detection Kit (Millipore Corp., Bedford, MA, USA) according to the manufacturer's protocol. Slides were then counter stained with hematoxylin QS (Vector Laboratories), mounted on slides and screened with a Nikon epifluorescent microscope (Nikon Eclipse 80i).

MTT cell proliferation assay. HUVECs were grown in 24 well plates in culture conditions as described above and each tested condition was done in triplicates. Cells were treated daily with PBS, 1 mM and 10 mM simvastatin for 3 and 5 days. On the final treatment day, 80 μL of 5 mg/mL thiazolyl blue tetrazolium bromide (MTT) were added to each well. Cells were incubated for 3.5 hours at 37˚C in culture hood. Media was carefully removed, and 600 μL MTT solvent (4 mM HCl, 0.1% NP40 in isopropanol) were added to each well. Well plates were covered with tinfoil and placed on an orbital shaker for 15 minutes. Media and cells from each well were carefully transferred to clear glass vials and final absorbance was spectrophotometrically measured at 570 nm absorbance to determine cell proliferation.

^{3}H-Thymididne incorporation assay. GL-26 cells were cultured in 6-well plates for 3 days to produce a 80-90% confluent layer in media containing DMEM with 1% penicillin/streptomycin, and 10% fetal calf serum (Gibco). Three days later, when the confluent layer was obtained, cells were washed from old media twice by adding 1 × PBS, then fresh media were added with either 1 or 10 μM purified active simvastatin (sodium salt; CalBiochem) or with vehicle (PBS only). 1 μCi/ml of ^{3}H-thymidine (Amersham, Arlington Heights, IL, USA) was added to into media of the plated cells for six hours. The media was then aspirated and cells were rinsed with PBS and subsequently lysed with 5% trichloroacetic acid (Aldrich Chemical Company, Milwaukee, WI, USA) at 4˚C. Cells were fixed with 70% ethanol and solubilized with 0.2 N NaOH. The solute was collected in InstaGel (Packard, Meriden, CT, USA) prior to counting.

Qualitative 3-D angiogenesis. HUVECs were seeded onto gelatin-coated cytodex microcarriers (MCs) to a final density of approximately 30 cells/bead and maintained in large volume of M199 medium with 4 mM glutamine, 50 mg/ml heparin and 2.5 μg/ml of endothelial cell growth supplement-ECGS for 2-4 days at 37˚C. Prior to placing the cells into 24-well plates, cell-coated MCs were then added into fibrin gel and allowed to set with the addition of thrombin (0.625 U/ml). After clotting was complete, the fibrin gel was equilibrated with M199 medium for 2 hours. Fresh media was changed after 2 hours, and embedded cells on the fibrin gel were cultured up to 3 days to allow angiogenic development. Cells were treated either 1 μM purified active simvastatin and/or 50 ng/ml recombinant human VEGF$_{165}$ (Intergen Co., NY, USA). The vessel formation was scored at day 8.

Results

GL-26 tumor model in vivo. All tumor-bearing animals became moribund between POD 29 and 35 (Figure 1A). The average survival time for control animals was 32.6±2.19 days, 29.8±0.84 days and 30.2±0.84 days for animals treated with low-dose and high-dose simvastatin, respectively. Compatible changes in tumor size were observed within this
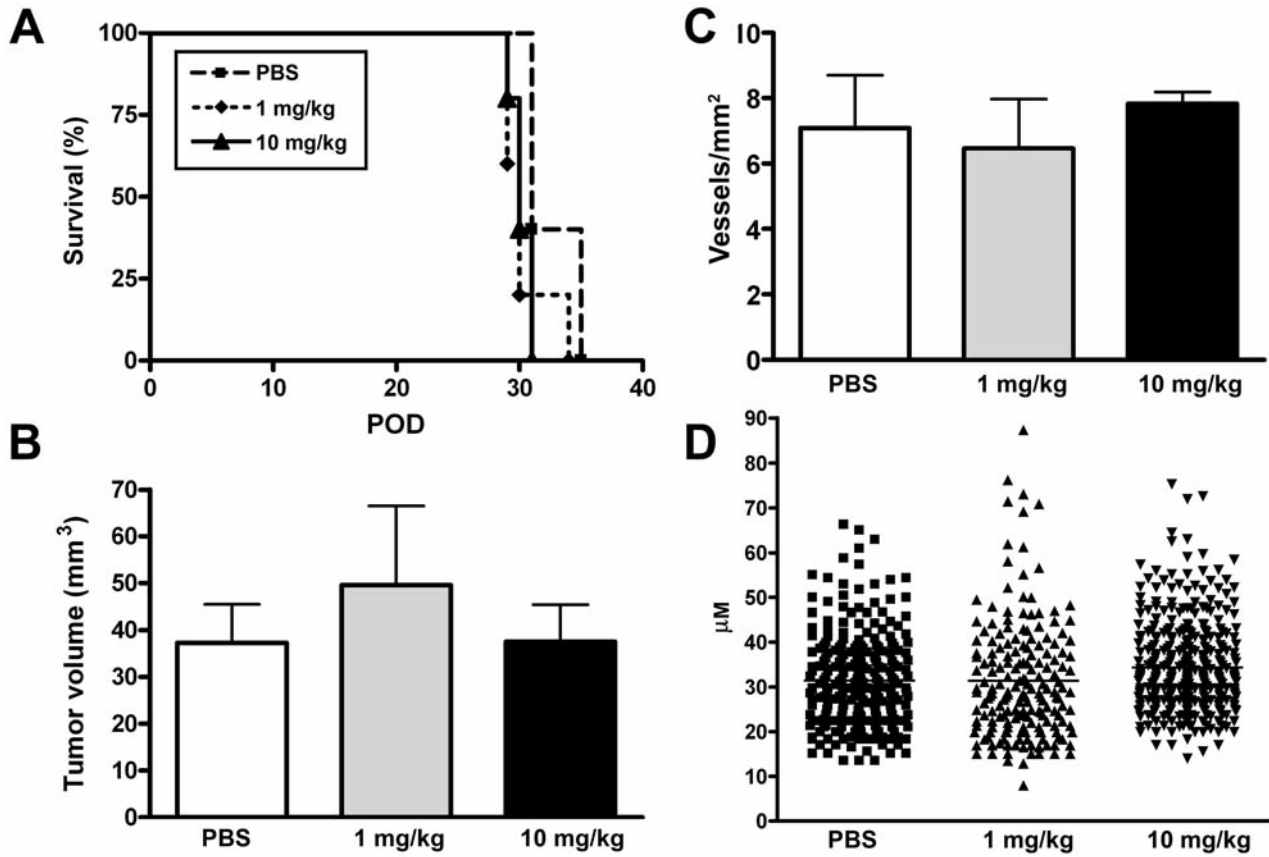
Figure 1. *Survival of animals treated with PBS (control), low-dose and high-dose simvastatin (A). The average survival after surgery was 32.6±2.2 days, 29.8±0.8 days and 30.2±0.8 days in control, low-dose and high-dose simvastatin-treated animals, respectively (POD, postoperative day). Average tumor size (mm³) of animals at time of sacrifice (B) was 37.23±16.45 mm³, 49.61±33.84 mm³ and 37.46±17.84 mm3 in control, low-dose, and high-dose simvastatin-treated mice, respectively. Average vascular density (vessels/mm²) of these animals (C) was 23.59±9.33 vessels/mm², 21.52±8.68 vessels/mm² and 26.09±2.37 vessels/mm² in control, low-dose and high-dose simvastatin-treated mice, respectively. Average vessel caliber (μm) of moribund animals (D) was more pronounced in the high-dose simvastatin group (34.4±10.4 μm), compared to both control (31.4±10.6 μm, p<0.001, Mann-Whitney test), and low-dose simvastatin (31.4±13.3 μm, p<0.0001, Mann-Whitney test) groups.*

time course. It was shown that the tumor size in the control group was 7 mm³ on POD 10, which reached to 37.2±16.4 mm3 when they became moribund. There was no statistical significance in difference of tumor size when compared to animals treated with low-dose (49.6±33.8 mm³) and high-dose (37.5±17.8 mm³) simvastatin (Figure 1B).

High-concentration simvastatin increased vessel caliber. A concomitant increase in tumor vascular density was noted in the control group, from 10 vessels/mm² (POD 15) to 23.6±9.33 vessels/mm² (POD 32). A similar increase in vascular density was noted in the low-dose (21.5±8.68 vessels/mm²) and high-dose (26.1±2.37 vessels/mm²) simvastatin-treated animals (Figure 1C) during this period of tumor growth. At the same time, vessel caliber had more than tripled from approximately 7 μm on POD 15 to 31.4±10.6 μm (POD 32) in the control group, and 31.4±13.3 μm and

34.4±10.4 μm in the low-dose and high-dose simvastatin treatment groups, respectively (Figure 1D). The caliber and aberrance of their morphology were more pronounced in the high-dose simvastatin-treated group, compared to both control (*p*<0.001, Mann-Whitney test) and low-dose simvastatin-treated (*p*<0.0001, Mann-Whitney test) groups, showing more erratic behavior of tumor vasculature at this phase of tumor proliferation.

Low-concentration simvastatin increased necrosis and apoptosis. Simvastatin did not provide an overall advantage in survival, tumor size or vascular density. However, different drug concentrations seemed to affect distinct tumor characteristics. Necrosis was more noticeable in animals that had been treated with low-dose simvastatin. A larger necrotic cavity was seen in these animals (8.74±7.54 mm³), as compared to both control (0.82±0.37, *p*<0.05, Student's *t*-test)
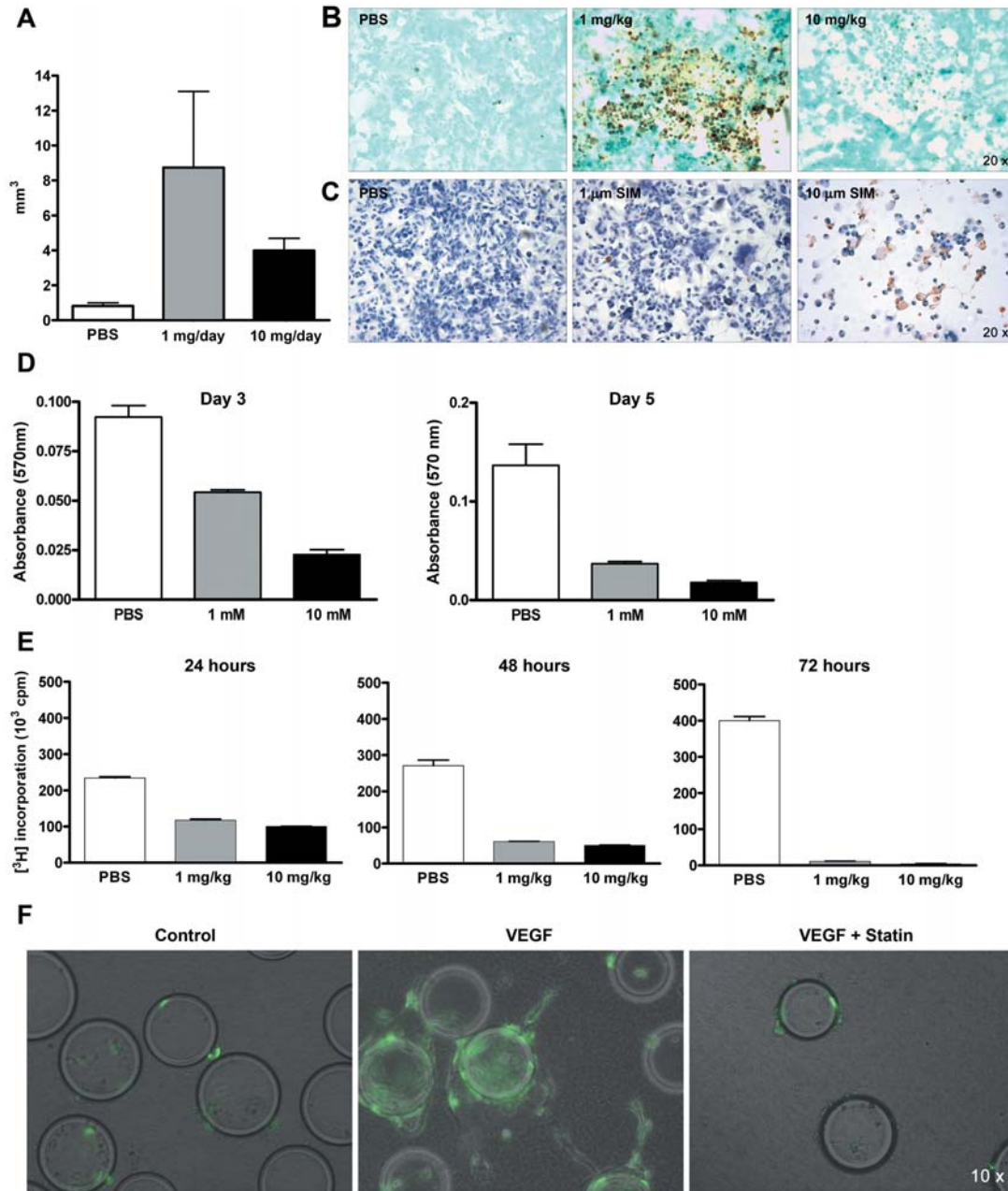
Figure 2. *Average necrotic cavity volume (mm³) at time of sacrifice (A) was found to be significantly larger in the low-dose simvastatin group (8.74±7.54 mm³) compared to both control (0.82±0.37; p<0.05, t-test) and high-dose simvastatin (3.98±1.40; p<0.05, t-test) groups. In vivo TUNEL analysis (B) (cells/20 × field view area) showed that low-dose simvastatin induced significantly more (325.5±255.1 cells) apoptosis compared to both control (21.0±8.25 cells; p<0.0001, t-test) and high-dose simvastatin (46.5±14.1 cells; p<0.0001, t-test) groups. All magnifications, ×20. Induced apoptosis of GL-26 tumor cell line following simvastatin treatment in vitro (C) reveals that simvastatin inhibited GL-26 cell growth in culture and induced apoptosis in a dose-dependant manner. GL-26 cell line treated with media only (PBS, left), 1 μM of simvastatin (SIM, middle), and with 10 μM of SIM (right). All treatments were harvested after 24 h, and images are representative of 3 replicates from each treatment. All magnifications, ×20. Day 3 MTT proliferation assay revealed that absorbance in 1 mM (0.05±0.01) and 10 mM (0.02±0.01) statin treatments reduced proliferation compared to control (0.09±0.01, p<0.0001) (D). Similarly, day 5 assay showed a similar trend with absorbance in 1 mM (0.04±0.01) and 10 mM statin (0.02±0.01) treatments, compared to control (0.14±0.04, p<0.01) In vitro ³H-thymididne incorporation at 24, 48, and 72 h (E). At 24 h, high-dose simvastatin caused a significant decrease in ³H-thymididne incorporation (100.2×10³±366 pcm) compared to both control (234.2×10³±4082 pcm; p<0.001, t-test) and low-dose simvastatin treatment groups (117.3×10³±3915 pcm; p<0.05, t-test). A similar trend was observed at 48 h (compared to both control, p<0.005, and low-dose simvastatin, p<0.01), and at 72 h (compared to both control, p<0.001, and low-dose simvastatin, p<0.05). Qualitative 3-D culture by seeding HUVECs onto gelatin-coated cytodex microcarrier and maintained in fibrin gel (F). Proliferation of HUVECs was markedly enhanced by VEGF (center panel) as compared to control (left); however, this effect was negated in the presence of a low concentration of simvastatin (1 μM).*
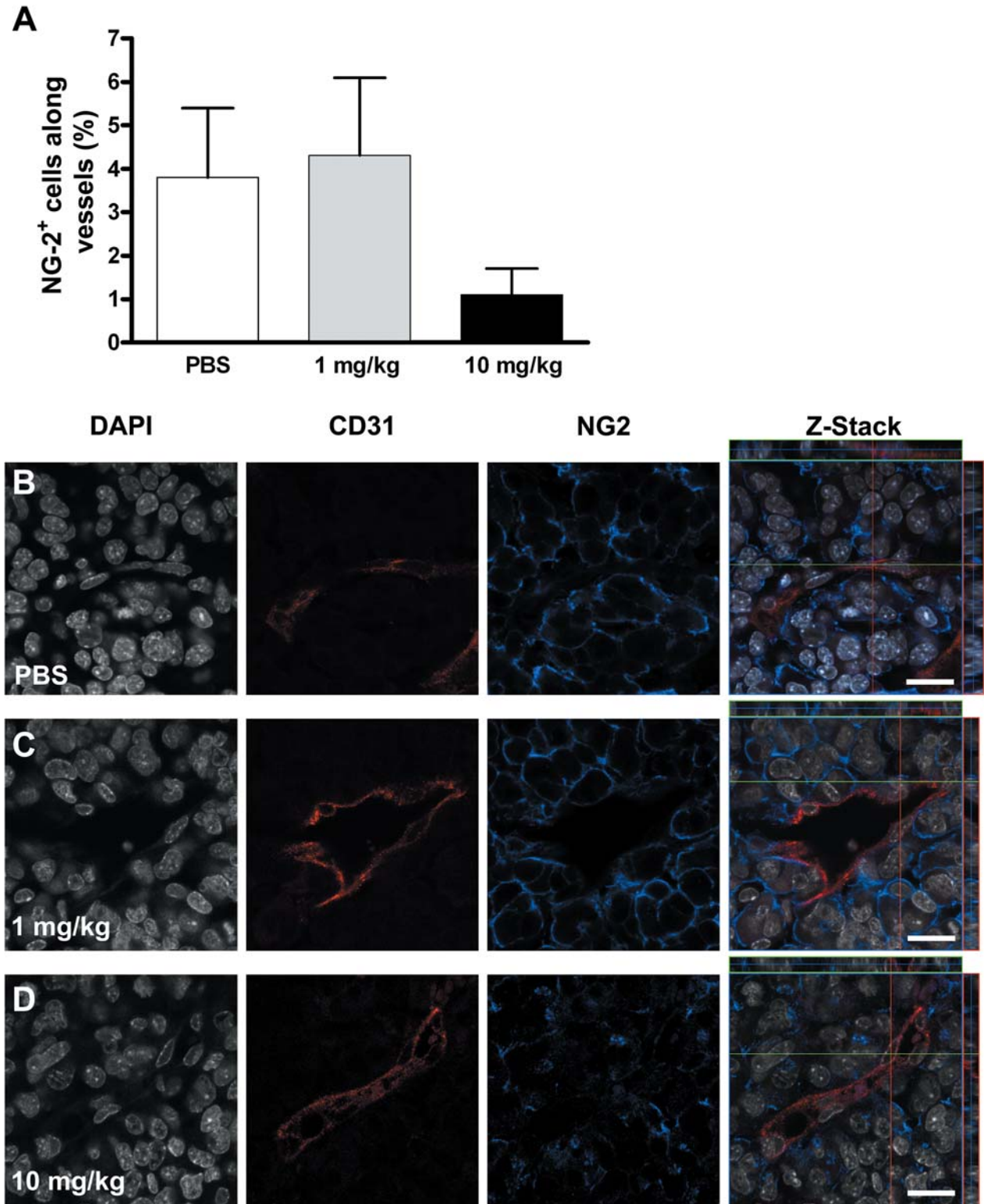
Figure 3. *High-dose simvastatin reduced the proportion of NG-2$^+$ pericytes along the tumor angio-architecture (A) (1.1±0.6%) as compared to both control (4.3±1.8%) and low-dose simvastatin (3.8±1.6%) groups (p<0.05, ANOVA). These NG-2$^+$ cells were localized along CD31$^+$ blood vessels of control (B), low-dose (C), and high-dose (D) simvastatin groups, and had the appropriate morphology and perivascular proximity to endothelial cells (CD31) as depicted in the Z-stack analysis. Additionally, these panels illustrate that there was a decrease in pericytic cells in high-dose simvastatin as compared to control and low-dose simvastatin, implying an inversely proportional dose-dependent effect of simvastatin. Scale bars, 20 μm.*

and high-dose simvastatin-treated (3.98±1.40, $p<0.05$, Student's t-test) groups (Figure 2A). In addition, there was a difference in the distribution of the vascular caliber and arborization of these vessels. *In vivo* TUNEL assay performed on the three different treatment groups showed that low-dose simvastatin induced significantly more apoptosis compared to both control ($p<0.0001$, t-test) and high-dose simvastatin-treatment ($p<0.0001$, t-test) groups (Figure 2B). *In vitro* ^{3}H-thymididne incorporation assay suggested that simvastatin exhibits a dose-dependent inhibition of GBM (Figure 2C) and human endothelial cell proliferation (Figure 2D). We noticed a significant decrease in proliferation in human endothelial cells in culture after they had been exposed to 1 mM and 10 mM of simvastatin ($p<0.01$). Similarly, when GL-26 cells were subjected to these concentrations of simvastatin, they also showed a compatible decrease in proliferation at 24, 48 and 72 hours (Figure 2E).

Additionally, a qualitative 3-D culture revealed that simvastatin markedly abolished the effect of VEGF in inducing tubular formation in HUVECs (Figure 2F). However, in comparing the proliferation of HUVECs and GL-26 cells, the effect of low-concentration simvastatin was less dramatic on the apoptosis of GL-26 cells *in vitro*. These results may indicate that at lower doses, simvastatin induces necrosis and apoptosis in mouse GBM, while higher doses seem to halt proliferation more efficiently and may affect vascular density and caliber.

High-dose simvastatin treatment increased vessel caliber by reducing the number of pericytic cells along the tumor vessel wall. High-dose simvastatin reduced the number of CD31 (endothelial cells) *in vivo*, but most importantly, it significantly reduced the number of perivascular NG-2^{+} cells along the vascular tree (1.1±0.6%) as compared to both control and low-dose simvastatin treatment ($p<0.05$, ANOVA) groups (Figure 3A-D). Tumors treated with low-dose simvastatin also showed a reduction in the pericyte counts (3.8±1.6%), although this was not significantly different from that of controls (4.3±1.8%). This dose-dependent effect on pericytes might explain the increase in vessel caliber that was found in tumors that had been treated with high-dose simvastatin.

Discussion

Although the exact mechanism of the tumorolytic effect of statins has not yet been elucidated, several plausible mechanisms have been proposed. Prasanna *et al.* suggest that dependence of malignant gliomas on the mevalonate pathway for cell replication may be the reason for the effects of statins on these tumors (15). It has also been suggested that other statins may increase the expression of the peroxisome proliferator-activated receptor, which functions as a transcription factor involved in the control of lipid metabolism, cell growth and differentiation (15). Bhat *et al.* demonstrated that astrocytic differentiation may be stimulated by reduced cholesterol levels, which provides an alternative mechanism of statin action (16). Other studies indicate that some statins disrupt organization of actin stress fibers, thus inhibiting migration, probably through focal adhesion kinase (17). Jakobisiak *et al.* have suggested that statins interact with Ras (18) and Rho pathways and inhibit the cyclin-dependent kinase pathway (1). Isoprenol levels and mitogen-activated protein kinase also seem to be affected by some statins, potentially affecting GBM proliferation and inducing apoptosis (18).

Here, we investigated the effects of simvastatin on an orthotopic mouse GBM model with an emphasis on the tumor cells and the associated vascular architecture. Our results show that simvastatin promoted apoptosis *in vivo* and *in vitro*. Its pro-apoptotic effect was more noticeable when the drug was given at a low dose. There was a profound effect on the tumor dropout, as demonstrated in having a larger area of empty space within the tumor mass, despite the lack of overall changes in tumor size between animals that were treated with PBS and high-dose simvastatin. Interestingly, simvastatin also inhibited the proliferation of GL-26 cells *in vitro*, as demonstrated by the ^{3}H-thymididne incorporation assay. This antiproliferative effect was more pronounced at a high dose of the drug. This antiproliferative effect of simvastatin is most likely mediated by the inhibition of the Ras and Rho pathways (18).

Tumor proliferation and tumor expansion are causally linked with neo-vascularization. Statins seem to have a biphasic effect on angiogenesis. At low nanomolar concentrations, statins activate the phosphatidylinositol 3-AKT kinase pathway, resulting in phosphorylation of endothelial nitric oxide synthase, which is a critical mediator of proliferation in endothelial cells (19). However, at a 10 μM dose, an antiproliferative effect on endothelial cells has been reported (20). The down-regulation of the Raf/MEK/ERK pathway is thought to be the root cause of the inhibitory effect of statins on endothelial-cell proliferation (21). In our *in vivo* model, simvastatin did not significantly affect the mean vascular density. However, it is of interest that there was a large variance in the distribution of vascular density among the sections from tumors that were treated with PBS and low-dose simvastatin ($p<0.03$, F-test). This pattern is commonly seen in tumors with ongoing angiogenesis. In general, tumor vessels are abnormal in terms of having disorganized morphology and larger caliber. This aberrant appearance is attributed in part to the fragmentation of the basal lamina and dissociation of mural pericytic cells. This is reflected in the wide distribution of the vascular caliber as observed *in vivo* when the animals were treated with low-dose simvastatin. However, at a higher simvastatin dose, we found that the vessels were of an even

larger caliber and of a more sinusoidal appearance. Additionally, we note a reduction in the number of endothelial cells within the tumor vascular tree, which is independent of the simvastatin dosage used in this study. Conversely, the effect of dose dependence is more prominently observed in the vascular auxiliary cells, the pericytes. The proportion of NG-2^{+} cells in the statin treatment groups was significantly less than in control samples. We surmise that at a low dose, simvastatin affects tumor apoptosis but does not affect angiogenesis to a great degree. At a higher dose, simvastatin indirectly halts angiogenesis by promoting vascular disintegration and possibly apoptosis of the mural pericytes. Weis *et al*. (22) showed that a 0.5 mg/kg/day dose of cervastatin did not affect human adult dermal microvascular cells, but a 2.5 mg/kg/day dose blocked inflammation-induced angiogenesis, reduced vascular proliferation and reduced VEGF release. Likewise, at this dosage, Weis *et al*. were able to demonstrate that cervastatin reduced vascular density and tumor size in a subcutaneous lung cancer model. Collectively, low-dose simvastatin affected the proliferation of tumor and endothelial cells in a dose dependent manner, which resulted in the cavitation of the tumor mass found in animals.

Additionally, high-dose simvastatin treatment reduced the number of pericytes along the tumor vascular tree in our tumor model. This concurs with the finding of Boucher *et al*. (9) who showed that simvastatin promoted apoptosis in primary pericyte cultures. This process was thought to be mediated by capase-3 and -7. Furthermore, Boucher *et al*. showed that cholesterol can partially reverse this process. They concluded that simvastatin affected lipid raft components such as caveolin-1 within the cell membrane. We would like to extend their hypothesis by suggesting that simvastatin alters the lipid raft within the membrane of pericytes and indirectly perturbs the interaction between these mural cells and the endothelial cells. Thus, the resulting vessels are more chaotic in their appearance and integrity. As a result, the animals succumbed to an increase in cerebral edema and intratumoral hemorrhage. This paradoxical effect of high-dose simvastatin on tumor proliferation and vascular disintegration underpins the idea put forth by Folkman (23) and Jain *et al*. (24) that any situation that promotes the de-normalization of tumor vasculature may potentially facilitate tumor colonization, and may be counterproductive and/or harmful for ongoing therapy.

Intuitively, metronomic administration of statins should be beneficial, as demonstrated in the reduction of cancer incidence in patients whom have been on statins for hypercholesterolemia (25). Unfortunately, the effect of statins is diverse and multifaceted, while the opposing effects of statins at various doses makes their use as adjuvant therapy in treating brain tumors more difficult. A multicenter prospective study using simvastatin in recurrent brain tumor may help to define the efficacy of this therapy.

References

1 Jakobisiak M and Golab J: Potential antitumor effects of statins (Review). Int J Oncol *23(4)*: 1055-1069, 2003.

2 Gliemroth J, Zulewski H, Arnold H and Terzis AJ: Migration, proliferation, and invasion of human glioma cells following treatment with simvastatin. Neurosurg Rev *26(2)*: 117-124, 2003.

3 Murakami M, Goto T, Saito Y *et al*: The inhibitory effect of simvastatin on growth in malignant gliomas – with special reference to its local application with fibrin glue spray *in vivo*. Int J Oncol *19(3)*: 525-531, 2001.

4 Kikuchi T, Nagata Y and Abe T: *In vitro* and *in vivo* antipro-liferative effects of simvastatin, an HMG-CoA reductase inhibitor, on human glioma cells. J Neurooncol *34(3)*: 233-239, 1997.

5 Soma MR, Baetta R, Bergamaschi S *et al*: PKC activity in rat C6 glioma cells: changes associated with cell cycle and simvastatin treatment. Biochem Biophys Res Commun *200(2)*: 1143-1149, 1994.

6 Soma MR, Baetta R, De Renzis MR *et al*: *In vivo* enhanced antitumor activity of carmustine [*N,N*'-bis(2-chloroethyl)-*N*-nitrosourea] by simvastatin. Cancer Res *55(3)*: 597-602, 1995.

7 Soma MR, Pagliarini P, Butti G *et al*: Simvastatin, an inhibitor of cholesterol biosynthesis, shows a synergistic effect with *N,N*'-bis(2-chloroethyl)-*N*-nitrosourea and beta-interferon on human glioma cells. Cancer Res *52(16)*: 4348-4355, 1992.

8 Klement H and Rak J: A disconnect between antitumor and antiangiogenic effects of fluvastatin *in vitro* and *in vivo*. Neoplasma *53(2)*: 111-118, 2006.

9 Boucher K, Siegel CS, Sharma P *et al*: HMG-CoA reductase inhibitors induce apoptosis in pericytes. Microvasc Res *71(2)*: 91-102, 2006.

10 Asakage M, Tsuno NH, Kitayama J *et al*: 3-Hydroxy-3-methylglutaryl-coenzyme A reductase inhibitor (pravastatin) inhibits endothelial cell proliferation dependent on G_1 cell cycle arrest. Anticancer Drugs *15(6)*: 625-632, 2004.

11 Santarelli JG, Udani V, Yung YC *et al*: Incorporation of bone marrow-derived Flk-1-expressing CD34^{+} cells in the endothelium of tumor vessels in the mouse brain. Neurosurgery *59(2)*: 374-382, 2006.

12 Werner M, Sacher J and Hohenegger M: Mutual amplification of apoptosis by statin-induced mitochondrial stress and doxorubicin toxicity in human rhabdomyosarcoma cells. Br J Pharmacol *143(6)*: 715-724, 2004.

13 Taraseviciene-Stewart L, Scerbavicius R, Choe KH *et al*: Simvastatin causes endothelial cell apoptosis and attenuates severe pulmonary hypertension. Am J Physiol Lung Cell Mol Physiol *291(4)*: L668-676, 2006.

14 Veeravagu A, Hou LC, Hsu AR *et al*: The temporal correlation of dynamic contrast-enhanced magnetic resonance imaging with tumor angiogenesis in a murine glioblastoma model. Neurol Res *30(9)*: 952-959, 2008.

15 Prasanna P, Thibault A, Liu L and Samid D: Lipid metabolism as a target for brain cancer therapy: synergistic activity of lovastatin and sodium phenylacetate against human glioma cells. J Neurochem *66(2)*: 710-716, 1996.

16 Bhat NR and Volpe JJ: Relation of cholesterol to astrocytic differentiation in C-6 glial cells. J Neurochem *42(5)*: 1457-1463, 1984.

17 Obara S, Nakata M, Takeshima H *et al*: Inhibition of migration of human glioblastoma cells by cerivastatin in association with focal adhesion kinase (FAK). Cancer Lett *185(2)*: 153-161, 2002.

18 Bouterfa HL, Sattelmeyer V, Czub S *et al*: Inhibition of Ras farnesylation by lovastatin leads to down-regulation of proliferation and migration in primary cultured human glioblastoma cells. Anticancer Res *20(4)*: 2761-2771, 2000.

19 Pirillo A, Jacoviello C, Longoni C *et al*: Simvastatin modulates the heat-shock response and cytotoxicity mediated by oxidized LDL in cultured human endothelial smooth muscle cells. Biochem Biophys Res Commun *231(2)*: 437-441, 1997.

20 Negre-Aminou P, van Vliet AK, van Erck M *et al*: Inhibition of proliferation of human smooth muscle cells by various HMG-CoA reductase inhibitors; comparison with other human cell types. Biochim Biophys Acta *1345(3)*: 259-268, 1997.

21 Wu J, Wong WW, Khosravi F *et al*: Blocking the Raf/MEK/ERK pathway sensitizes acute myelogenous leukemia cells to lovastatin-induced apoptosis. Cancer Res *64(18)*: 6461-6468, 2004.

22 Weis M, Heeschen C, Glassford AJ and Cooke JP: Statins have biphasic effects on angiogenesis. Circulation *105(6)*: 739-745, 2002.

23 Folkman J: Angiogenesis: an organizing principle for drug discovery? Nat Rev Drug Discov *6(4)*: 273-286, 2007.

24 Jain RK, di Tomaso E, Duda DG *et al*: Angiogenesis in brain tumours. Nat Rev Neurosci *8(8)*: 610-622, 2007.

25 Kumar AS, Benz CC, Shim V *et al*: Estrogen receptor-negative breast cancer is less likely to arise among lipophilic statin users. Cancer Epidemiol Biomarkers Prev *17(5)*: 1028-1033, 2008.